Eur Radiol (2002) 12:814–823
DOI 10.1007/s003300101128

Maria Cova
Renato Toffanin

MR microscopy of hyaline cartilage: current status

Received: 5 June 2001
Accepted: 17 August 2001
Published online: 11 October 2001

M. Cova (✉)
Department of Radiology,
University of Trieste,
Ospedale di Cattinara,
Strada di Fiume 447, 34149 Trieste, Italy
e-mail: cova@gnbts.univ.trieste.it
Tel.: +39-040-3994372
Fax: +39-040-3994500

R. Toffanin
Department of Biochemistry,
Biophysics and Macromolecular Chemistry,
Via L. Giorgieri 1, 34127 Trieste, Italy

R. Toffanin
PROTOS Research Institute, P.O. Box 972,
34100 Trieste, Italy

Abstract Cartilage degenerative diseases, such as osteoarthritis, affect million of people. Magnetic resonance imaging is presently the most accurate imaging modality in evaluating the state of hyaline cartilage; however, clinical MRI does not accurately reveal early degenerative alterations in cartilage, due mainly to low spatial resolution. Magnetic resonance microscopy (MRM, or μMRI) appears exceptionally well suited to the in vitro or ex vivo study of this heterogeneous tissue, due to its high spatial resolution; however, despite this, further studies are necessary to evaluate the potential of MRM in the detection of early cartilage damage. Herein we briefly review the current applications of MRM in the study of hyaline cartilage. In particular, we review the MR appearance of hyaline cartilage on high-resolution images, the different MRM techniques used to image normal and enzymatically or chemically degraded cartilage and the potential use of contrast agents. The future directions and the relevance of MRM findings for a better understanding of cartilage physiology in health and disease are also discussed.

Keywords Cartilage · MR imaging · MR microscopy · Review

Introduction

The most common cause of hyaline articular cartilage damage is osteoarthritis, either primary or due to trauma. It is estimated that currently within Europe there are 150,000 individuals with traumatic defects of the knee cartilage. In total there are 30 million Europeans that suffer from osteoarthritis. Since this degenerative disease affects mainly people over the age of 40 years, in Europe the number of middle-aged and elderly people suffering cartilage diseases is set to rise dramatically in the coming years. For this reason, the use and development of new methodologies for cartilage evaluation are a key issue for a better understanding and treatment of the degenerative process of articular cartilage. Morphological and biochemical information can be obtained by MRI, which is presently the most accurate imaging modality in evaluating the state of hyaline cartilage [1, 2]; however, clinical MRI does not accurately reveal early degenerative alterations in articular cartilage, due mainly to low spatial resolution [3]. Magnetic resonance microscopy (MRM, or μMRI) appears exceptionally well suited to the in vitro or ex vivo study of this heterogeneous tissue, due to its high spatial resolution [4]; however, despite this, further studies are necessary to evaluate the potential of MRM in the detection of early cartilage damage.

In this review we describe the MR appearance of hyaline cartilage on high resolution images, the different MRM techniques used to image normal and enzymatically or chemically degraded cartilage and the potential use of contrast agents. The future directions and the relevance of MRM findings for a better understanding of cartilage physiology in health and disease are also discussed.

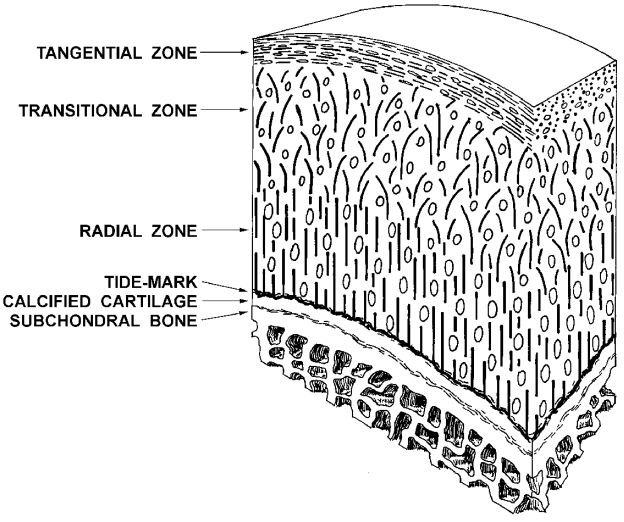

Fig. 1 Histological zones in hyaline cartilage. It is shown that collagen fibres are parallel to the surface in the superficial (tangential) zone, curved in the intermediate (transitional) zone and perpendicular to subchondral bone in the deep (radial) zone

Fig. 2 Spin-echo image of human knee cartilage (TR/TE: 1800/20 ms). A trilaminar appearance of the femoral condyle hyaline cartilage is shown (*arrows*). The superficial lamina is hypointense, the intermediate lamina is hyperintense and the deep lamina is hypointense

Hyaline cartilage

Hyaline or articular cartilage consists of chondrocytes and a supportive matrix composed of water, proteoglycans and a collagen-fibres framework. Depending on the different arrangement and orientation of the cellular component and the collagen framework, cartilage histology shows a trilaminar pattern (Fig. 1): a superficial layer or tangential zone; an intermediate layer or transitional zone; and a deep layer or radial zone. In the tangential zone the collagen fibres are densely packed and oriented parallel to the articular surface, whereas in the intermediate zone the collagen fibres have a random or oblique orientation. The radial zone represents the major part of the cartilage thickness with large collagen fibres oriented perpendicularly to the joint surface. The deepest part of the inner layer, adjacent to the subchondral bone, is partially calcified. The area that corresponds with the boundary between calcified and uncalcified cartilage is called "tidemark" region. Also the amount of water and proteoglycans differs among the cartilage layers, as water concentration is greater in the tangential zone whereas proteoglycans concentration is greater in the transitional zone.

The function of hyaline cartilage as a load-bearing tissue and its ability to undergo reversible deformation depend on the specific organisation of the macromolecular components in the extracellular matrix. In particular, the arrangement of the collagen fibres into a stiff three-dimensional framework can balance the swelling pressure of the proteoglycan–water gel.

MRI and MRM appearance

Magnetic resonance imaging appears to be the most useful imaging technique for evaluation of articular cartilage [1]. It has long been known that hyaline cartilage shows a laminar structure on MR images (Fig. 2) [5, 6, 7, 8, 9, 10, 11, 12, 13], but there is some controversy on the total number of laminae and their appearance on MRI [12, 14, 15, 16]. For human articular cartilage, Modl et al. [6] reported a trilaminar appearance on both T1- and T2-weighted images with the superficial lamina of low signal intensity, the middle lamina of intermediate to high intensity and the band of low signal intensity at the bone–cartilage boundary. These authors suggested that the superficial lamina corresponded, although not in thickness, to the zone with the tangential orientations of collagen fibres. The middle lamina corresponded to the transitional layer with the random orientation of the fibres and the deepest lamina with lower intensity was assigned to the zone with radial orientation of the fibres and to the calcified zone of cartilage adjacent to the subchondral bone. The same trilaminar structure was reported by Chalkias et al. [8] on T1- and T2-weighted and gradient-echo images of disarticulated human femoral heads. The T1 and T2 relaxation times were also measured and resulted higher for the middle lamina than those measured for the deeper, markedly hypointense lamina. Recht et al. [7] reported the trilaminar appearance of cadaveric knee cartilage, however, with the intensities reversed in comparison with previous studies. A reversed pattern of signal intensities was also found by Lehner et al. [5] in a study of bovine patellar cartilage.

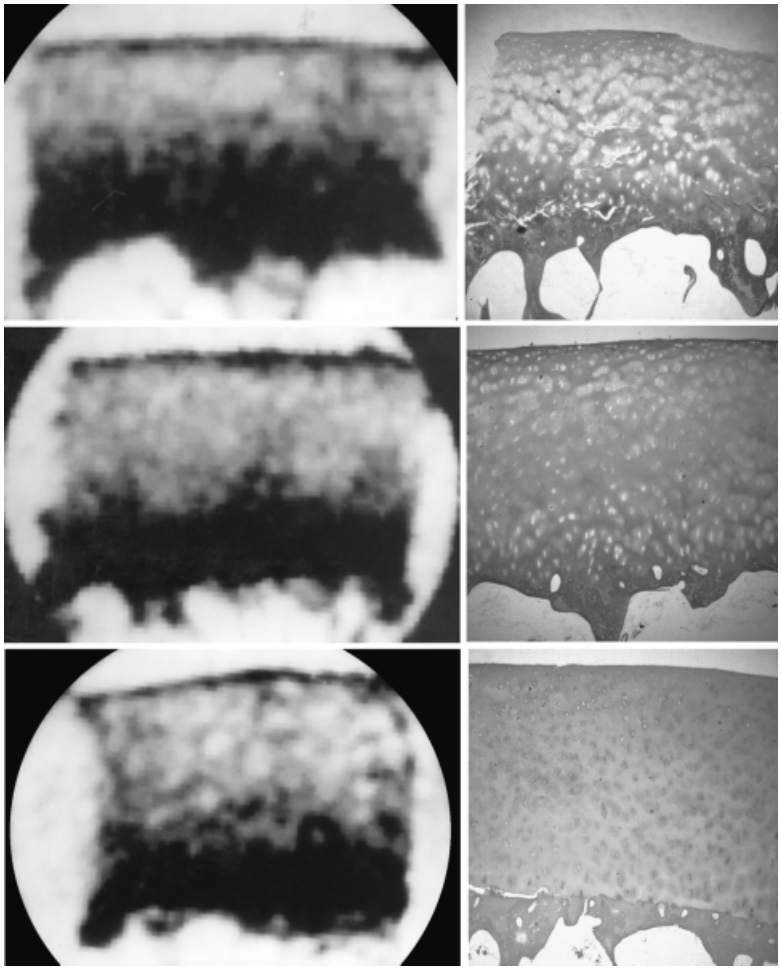

Fig. 3 Magnetic resonance microscopy images (*left*) and corresponding histology (*right*) of cartilage–bone plugs excised from different sites of a human femoral head. These images show that the hypointense superficial lamina of cartilage has a constant thickness, whereas the thickness of the hyperintense intermediate lamina varies in the different sites of the femoral head. The pixel resolution is 47 µm and the TE is 30 ms. (Reprinted with permission from [13])

On strongly T2-weighted images, the cartilage had a trilaminar appearance with a superficial lamina of high intensity, an intermediate lamina of lower intensity and a deep lamina of higher signal intensity. On strongly T1-weighted images the intensity of the superficial lamina was lower than that of the intermediate one.

On the T1-, T2- and proton-density-weighted images of bovine patellar cartilage, Rubenstein et al. [17] found a signal intensity pattern identical to that described by Lehner and coworkers [5] on T2-weighted images. Moreover, they documented that the appearance of cartilage was dependent on its orientation in relation to the direction of the static magnetic field B_0. At an angle of 55° they observed a homogeneous appearance of cartilage, the so-called magic-angle effect [18]. An even more complicated pattern was found by Xia et al. [19] in a study of canine articular cartilage by means of MRM. The moderately T2-weighted image of a cartilage–bone plug harvested from the humerus bone showed three laminae of higher signal intensity with two laminae of lower intensity sandwiched between them. On the images of animal cartilage, a fourth lamina of calcified cartilage adjacent to the subchondral bone is also sometimes noticeable [17, 20]. It has very low signal intensity and it is often impossible to distinguish it from the subchondral bone.

To explain contradictions related to the MR appearance of articular cartilage Mlynárik et al. [9] performed ex vivo studies on human and porcine articular cartilage by MRM and MRI. They found that the signal intensity patterns for human and porcine specimens were similar, but an extra lamina of low intensity was frequently present on the images of porcine cartilage. Cova et al. [13] reported in their ex vivo study at 47-µm resolution of normal human cartilage that the laminar structure has a topographic dependence. The hypointense superficial lamina had a constant thickness in the different sites of the femoral head, whereas the thickness of the hyperintense intermediate layer varied, being thicker in the habitually loaded sites (Fig. 3).

The above-reported findings show the variety of laminar appearance of articular cartilage on MR images. This discrepancy may result from the use of a wide range of imaging parameters, from the different resolution ap-

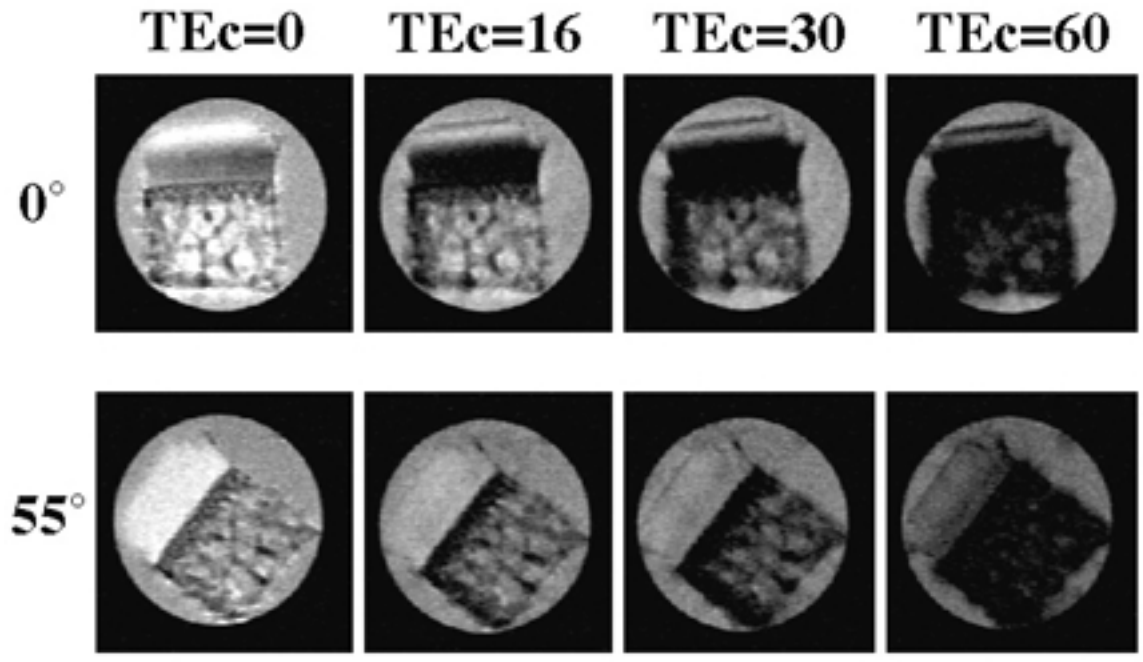

Fig. 4 Laminar appearance of hyaline cartilage and magic-angle effect. Proton spin-echo images of a canine cartilage-bone plug with the articular surface oriented at 0 and 55° with respect to the direction of the magnetic field B_0. The cartilage appears laminated at 0° and homogeneous at 55°. The pixel resolution is 14 µm and the contrast TE was between 0 and 60 ms. (Reprinted with permission from [15])

plied as well as from the use of different types of cartilage investigated (e.g. human and animal specimens, different joints, different sites in the same joint). The interpretation of the laminar appearance of articular cartilage on MR images can be further complicated by the presence of truncation artefacts. These artefacts can create a false laminar appearance in cartilage when using a fat-suppressed three-dimensional spoiled gradient-recalled sequence commonly used in clinical MR imaging [14, 21]. Erickson et al. [14] reported that the trilaminar appearance observed with the use of this specific sequence may be spurious and attributable to truncation artefacts. Frank et al. [21] published similar results and pointed out that truncation artefacts are responsible for the trilaminar appearance of cartilage on images of moderate resolution. The delineation of true cartilage laminae requires, therefore, high-resolution images and high signal-to-noise ratios.

In a recent study Xia [16] investigated the discrepancy in the laminar structure of cartilage by means of microscopic MR imaging experiments carried out at 14-µm pixel resolution on full-depth cartilage-bone plugs from several locations on the humeral head of two young healthy dogs. The study described a variable MR laminar appearance within the same humeral head and proved that laminar heterogeneity correlates with the spatial heterogeneity observed at a histological level and that this heterogeneity may be related to the load-bearing status of the tissue in the joint.

The results presented above clearly demonstrate that MRM may help clarify the complexity of cartilage laminae and help in the interpretation of moderate resolution images used in clinical MRI.

T2 relaxation anisotropy and magic-angle effect

As reported above, the truncation artefact can be a cause of false laminar appearance on MR images of articular cartilage when using fat-suppressed three-dimensional spoiled gradient-echo recalled sequences. A second artefact that is commonly found in articular cartilage when using T2-weighted images is the so called magic angle effect (Fig. 4) [15, 16, 17, 22]. This artefact produces increased signal and is found in articular cartilage because of its highly anisotropic arrangement of macromolecules, especially collagen. Magic angle refers to the angle-dependent increase in signal intensity resulting from increased T2 in anisotropic structures that is maximal at approximately 55° relative to the external magnetic field. Rubenstein et al. [17] presented evidence of magic-angle effects occurring in bovine hyaline cartilage. In their study on normal bovine patellar cartilage at 300-µm resolution they showed a loss of the trilaminar structure on spin-echo (SE) MR images when cartilage was oriented at 55° to the external magnetic field, i.e. in the direction of the minimum dipolar coupling. They concluded that the MRI appearance of the cartilage laminae is strongly influenced by the preferential alignment of water mole-

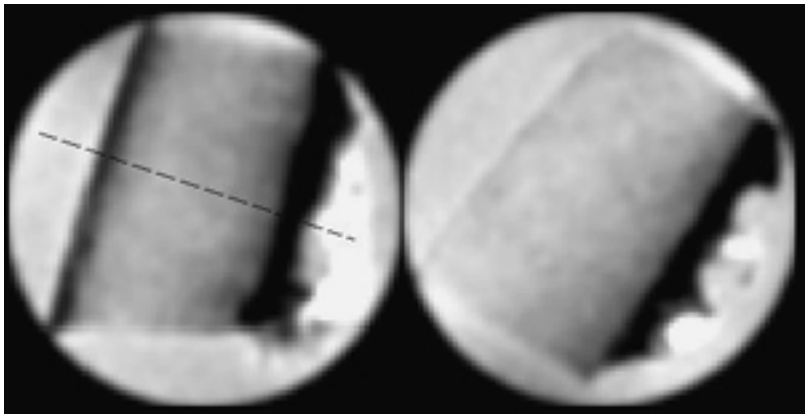

Fig. 5 Laminar appearance of hyaline cartilage. These two spin-echo images depict the same plug of human femoral cartilage measured under identical experimental conditions and with the articular surface parallel to the magnetic field B_0. The magic-angle effect invoked only by rotating the plug around its axis by approximately 90° demonstrates a nonuniform angular distribution of the collagen fibres within the superficial layer. The pixel resolution was 48 µm and the TE was 14 ms. (Reprinted with permission from [9])

cules associated with oriented collagen fibrils in the chondral tissue [23]. Mlynárik et al. [9] in a study on porcine and human cartilage by means of MRM supported the suggestion of Rubenstein and coworkers [17] that the proton dipolar interaction plays a significant role in the laminar appearance of articular cartilage. They also demonstrated a non-uniform angular distribution of the collagen fibres within the superficial layer (Fig. 5). The origin of the magic-angle effect on MR images of articular cartilage was investigated by Xia [24] on normal canine cartilage at 14-µm resolution. In this study Xia suggested that the T2 anisotropy in cartilage is closely associated with the spatial structure of the collagen fibrils meshwork. Gründer et al. [25] also demonstrated the angular dependence of signal intensity in cartilage explants from porcine femoral and humeral condyles. Gründer et al. [25] suggested a direct relation between the oriented collagenous structures and the anisotropic regions observed on MR images. Recently, Kim et al. [26] in a high-resolution study (voxel size 78×156×2000 µm) on bovine patella cartilage performed using a 1.5-T system showed an anisotropic angular dependency of the T2 mapping profile of cartilage from the magic-angle effect.

A few recent studies have also considered the MR appearance of hyaline cartilage under compressive force. Rubenstein et al. [27] studied the effects of compression and decompression on the MR imaging appearance of bovine articular cartilage. By obtaining consecutive spin-echo MR images (in-plane resolution up to 156 µm) of normal bovine cartilage with increments of pressure to a maximum of 4.14 MPa, they found that at short T2, low-signal-intensity lamina at the articular surface became thicker and more distinct. The signal intensity of the deep cartilage zone gradually decreased with increasing pressure and at maximum compression the cartilage showed uniform low signal intensity. After release of pressure, signal intensity changes on the MR images of cartilage were sequentially reversed. Rubenstein et al. [27] hypothesised that the variation of appearance and signal intensity of cartilage under pressure was due to a combination of net water loss and alteration in the collagen orientational structure. More recently, Gründer et al. [28] in a study performed on pig articular cartilage at 78-µm resolution proved that MR appearance of zones of radially and tangentially oriented collagenous fibres shows contrary changes under pressure. Rubenstein et al. [27] suggested that these changes can be explained by the variation of the grade of orientation of these fibres under pressure. They concluded that, based on these pressure-induced changes, new information about the biomechanical properties of articular cartilage can be obtained.

MRI and MRM techniques

Many MR techniques have been used to assess in vivo articular cartilage, with varying success. Both T1- and T2-weighted sequences have proved to be useful in the evaluation of hyaline cartilage. T2-weighted SE and fast SE sequences show cartilage abnormalities either as morphological defects on the surface or as high signal intensity abnormalities in the cartilage. The main advantage of using fast SE sequences is the relevant decrease in imaging time. Moreover, the use of fast SE sequences introduces magnetisation transfer contrast (MTC) on MR images, which may help in the detection of cartilage abnormalities. Magnetisation transfer contrast occurs in tissues with a high concentration of macromolecules [29] and collagen is the predominant responsible for the magnetisation transfer effect in articular cartilage. When collagen content is diminished, as in cartilage degradation, there is a decreased magnetisation transfer effect, resulting in increased signal intensity. Gradient-echo MR imaging with and without fat suppression has been used successfully in the detection of cartilage lesions, owing to the high-contrast delineation of cartilage [30]. The highest accuracy for clinical evaluation of cartilage has been obtained with T1-weighted

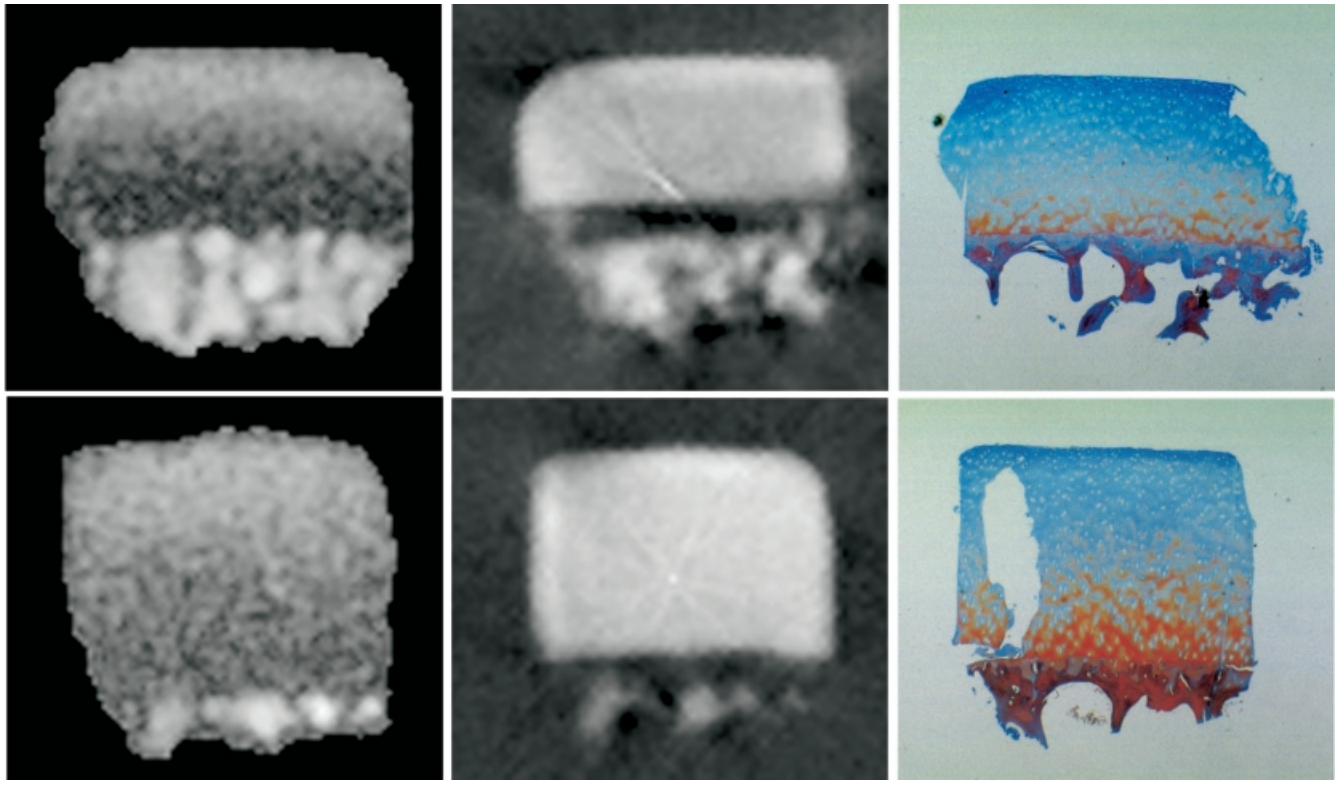

Fig. 6 Conventional spin-echo images (*left*), projection reconstruction (PR) spin-echo images (*middle*) and corresponding histology (*right*) of cartilage-bone plugs excised from the femoral head of a 78-year-old man. On the PR images acquired with a shorter echo time (TE=3.2 ms) the cartilage signal is increased compared with the conventional proton-density images (TE=30 ms), thus allowing an accurate delineation of the cartilage from the tidemark/cortical bone region. (Reprinted with permission from [34])

fat-suppressed three-dimensional spoiled gradient-echo images. The main advantage of fat suppression is the increase of the dynamic range of signal intensities in cartilage, allowing detection of more subtle changes in signal intensity [7]. The advantage of using three-dimensional gradient-echo imaging is the acquisition of contiguous thin-section images with a high signal-to-noise ratio [7, 31, 32]. The drawback of this sequence is the presence of truncation artefacts that can create a false laminar appearance in cartilage [14, 21]. Recently, Brossmann et al. [33] proposed a projection reconstruction (PR) MR imaging with an ultrashort TE (150 μs) for a better delineation of cartilage lesions. In their preliminary in vitro study at 0.625 mm resolution by using a 1.5-T MR imager, the PR approach proved to be superior to MTC subtraction and fat-suppressed 3D spoiled gradient-recalled acquisition in the steady-state MR imaging in the detection of cartilage abnormalities. The PR approach was also tested on porcine bone–cartilage explants by Cova et al. [34] by using a 7.05-T NMR instrument equipped with a microimaging accessory. In this study at 47-μm pixel resolution Cova et al. [34] compared the PR microimages with conventional SE microimages and with histology (Fig. 6). They showed that on 2D PR microimages acquired with an echo time of 3.2 ms the cartilage signal was increased, allowing an accurate delineation of cartilage from the tidemark/cortical bone region. The advantage of the PR method is that short TE can be used to obtain MR signal also from those structures with short T2 like the deep layer of articular cartilage. As a consequence, a more precise measurement of cartilage thickness compared with that performed by the conventional SE approach was feasible by using the PR method. They also showed an excellent correlation between PR microimages and histology (r=0.90). Short TE MRM was also used by Freeman et al. [10] to accurately measure the thickness of hyaline cartilage and determine the optimal MR contrast parameters for delineation of cartilage zones in normal human cartilage samples. Freeman et al. [10] examined cartilage samples at 9.4 T using 3D SE MR experiments to test the T2 relaxation loss in the deep layer of articular cartilage. Three-dimensional SE microimages were obtained at different TE, rging from a minimum of 1.5 ms to a maximum of 24 ms. They suggested that the T2 signal loss dominates the image contrast and, therefore, the accuracy of measuring cartilage by routine musculoskeletal MR imaging.

Although the above-reported studies were performed ex vivo on small tissue samples, short TE MRI methods should be applicable to clinical MR systems for the accurate measurement of the articular cartilage thickness. Further ex vivo and in vivo studies are required to assess their clinical potential in the evaluation of the extent and severity of osteoarthritis and in the response to drugs.

Pathomimetic studies and contrast agents

As recently pointed out by Rubenstein et al. [3] routine clinical MRI does not accurately reveal early degenerative changes in hyaline cartilage because of the moderate spatial resolution; only large defects and distorted changes in the signal intensity of the cartilage can be seen. On the other hand, MRM, thanks to its higher resolution, can help in the early detection and monitoring of cartilage degradation.

The early stages of degradation that occur before substantial changes in morphology are associated with changes in the concentration of proteoglycans and water, and in the organisation of collagen in the superficial layer of cartilage [3]. The role of enzymatic degradation in osteoarthritis is, however, not completely understood [35]. In particular, there is controversy about whether the degeneration of articular cartilage is initially caused by proteoglycan or collagen degradation. Over the past years pathomimetic interventions, either in vitro or in vivo, were performed by some authors to mimic the pathological changes in chemical composition of cartilage and to reveal correlation with MR parameters.

Proteoglycan depletion in articular cartilage was simulated by treating the tissue with enzymes or other agents in vivo and in vitro. Paul et al. [36] in their pioneer in vivo study on rabbit knees obtained T1-, PD- and T2-weighted images at 312-µm resolution after intra-articular injection of papain. They found that reduced articular cartilage thickness on the MR images of papain-treated knees corresponded to changes in cartilage proteoglycan content. More recently, MRM was used to monitor experimental osteoarthritis in the rat knee joint induced by iodoacetate [37]. This study proved the potential of high-field MRI in the investigation of ex vivo focal erosions of articular cartilage; however, no correlation was found between MR appearance and marked loss of proteoglycans. This finding was recently partially confirmed by Toffanin et al. [38] in their in vitro study on porcine articular cartilage explants. In this study 1D MR microscopy at 7.05 T was used to quantify the main MR parameters, such as T1 and T2 relaxation times, diffusion (D) and magnetisation transfer (M_s/M_0), on gradually proteoglycan-depleted cartilage. Toffanin et al. [38] found that only the longitudinal relaxation time T1 and the diffusion coefficient D were sensitive to an extensive proteoglycan depletion of the tissue. They concluded that further investigation on the macromolecular components (proteoglycans and collagen) of cartilage was necessary for a better understanding of the interaction mechanism between water and extracellular matrix that might lead to the early diagnosis of the cartilage damage by MRI.

The water diffusion coefficient in enzymatically degraded cartilage was also measured previously by other authors [39, 40]. Because hydration increases with cartilage degradation, the water diffusion coefficient was expected to monitor cartilage damage. Burstein et al. [39] showed that the diffusivity of water increased by 20% after treatment with trypsin (to remove the proteoglycans and noncollagenous proteins) and that diffusivity decreased upon compression of cartilage by 35%. Burstein et al. [39] suggested that water diffusion is dependent on the composition and density of the solid cartilage matrix. Xia et al. [40] treating canine cartilage explants with trypsin, hyaluronidase and collagenase found that the diffusion measurement can localise regions of cartilage degradation, but it is not sensitive to the content of the main macromolecular components of cartilage, i.e. proteoglycans and collagen. Therefore, although water diffusion can monitor nonspecific cartilage damage, water diffusion measurement alone appears not able to specifically reveal the loss of these macromolecules.

The proteoglycan loss in cartilage has also been evaluated by considering other parameters. For example, Duvvuri et al. [41] used $T1_\rho$ (T1 in the rotating frame) to monitor proteoglycans in normal and enzymatically degraded bovine articular cartilage. Duvvuri et al. suggested that $T1_\rho$ relaxation measurements are selectively sensitive to changes in proteoglycan concentration; however, further work is needed to fully investigate the mechanism of $T1_\rho$ relaxation in cartilage.

Some recent studies have shown that sodium magnetic resonance could be used to measure proteoglycans in normal and degraded cartilage [42] and that in vitro and in vivo sodium MR imaging could be used to visualise physiological [42, 43] and pathological changes [44, 45] in the proteoglycan concentration. Very recently Borthakur et al. [46] compared the results from sodium and proton MRI in detecting small changes in proteoglycan content in bovine articular cartilage specimens. In this study performed on partially proteoglycan depleted cartilage using a 4-T clinical MR system Borthakur et al. [46] showed that sodium MRI is both sensitive and specific in detecting small changes in proteoglycan concentration; however, considering the fact that several issues (e.g. sodium concentration, fast and slow T2 components, lower resolution) can confound the interpretation of the sodium MR images, methods using sodium MRI must be used with caution. With appropriate attention to varying relax-

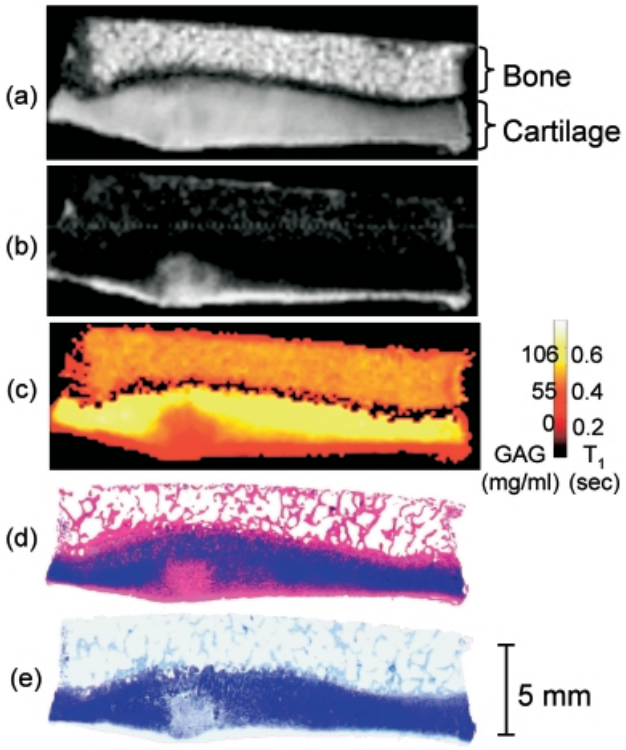

Fig. 7a–e Sample of human hyaline cartilage imaged at 8.45 T after equilibration with 1 mmol/l $Gd(DTPA)^{2-}$ and compared with subsequent histology. **a** Proton-density image, wherein the cartilage appears essentially intact. **b** T1-weighted MR image with an inversion time (TI) of 250 ms. Brighter areas are those with higher $Gd(DTPA)^{2-}$ and hence lower glycosaminoglycans. **c** Calculated T1 image, wherein the colour scheme reflects the absolute value of T1. **d** Hematoxylin and eosin staining confirms that the cartilage is anatomically intact and delineates the articular surface. **e** Toluidine blue staining, used as a specific stain for GAG, shows the lack of glycosaminoglycans on the cartilage surface and in the lesion. (Reprinted with permission from [42])

ation times across the sample, normalisation to water content and partial-volume effects, sodium MRI might provide quantitative information on the proteoglycan loss in cartilage disease.

In the past years, several authors have also investigated the influence of the collagen component on the MR parameters of articular cartilage. Kim et al. [47], using the proteoglycan and the collagen model systems as well as cartilage treated by chondroitinase AC II and trypsin, demonstrated a principal role of collagen in magnetisation transfer processes with little or no contribution from proteoglycans. Gray et al. [48] also reported changes in magnetisation transfer ratios in articular cartilage incubated in a trypsin solution and also in epiphyseal cartilage cultured with human recombinant interleukin-1β. They ascribed these changes to alterations in collagen organisation or in tissue structure. While the above studies suggested that collagen provides the main mechanism for MT in articular cartilage, in a more recent investigation Wachsmuth et al. [49] found that, in gradually proteoglycan-depleted cartilage, also proteoglycans may contribute to the MT effect; however, this effect is very small relative to the effect of collagen and therefore it may be difficult to use MT to monitor proteoglycan changes in cartilage disease.

A proton-based MR method for measuring proteoglycan changes in cartilage has recently been proposed [50, 51]. This method is based on the premise that the negatively charged contrast agent $Gd(DTPA)^{2-}$ will distribute in cartilage in inverse relation to the concentration of the negatively charged glycosaminoglycan (GAG) sidechains of proteoglycans. Figure 7 shows an example of the proton MR images of excised human cartilage samples obtained with this method to measure GAG concentration validated against histology. This method can also be used clinically after intravenous or intra-articular injection of $Gd(DTPA)^{2-}$ [52, 53].

Another method based on the GAG-dependent distribution of mobile ions has been proposed by Bacic et al. [54] who investigated in an animal model the applicability of a positively charged nitroxide as an MRI contrast agent in detection of the negatively charged proteoglycans within the cartilage.

Very recently, Wagner et al. [55] investigated at 7.01 T the influence of collagenase on the cartilage structure using polylisine-Gd-DTPA and liposome-entrapped contrast agents. After application of the above contrast agents, the collagenase-induced damage to the collagen network on the cartilage surface and the superficial cartilage zones was detected with great sensitivity.

Future directions

The list of the high-resolution MRI and MRM studies presented in this review is probably not exhaustive. The cited studies clearly indicate, however, that the magnetic properties of articular cartilage can be investigated in greater detail at microscopic resolution. In particular, high-resolution MRI and MRM, conducted in vitro or ex vivo and equally on animal models can provide new information on the physiology of articular cartilage in health and disease.

References

1. Disler DG, Recht MP, McCauley TR (2000) MR imaging of articular cartilage. Skeletal Radiol 29:367–377
2. Burstein D, Bashir A, Gray ML (2000) MRI techniques in early stages of cartilage disease. Invest Radiol 35:622–638
3. Rubenstein JD, Li JG, Majumdar S, Henkelman RM (1997) Image resolution and signal-to-noise ratio requirements for MR imaging of degenerative cartilage. Am J Roentgenol 169:1089–1096
4. Callaghan PT (1991) Principles of nuclear magnetic resonance microscopy. Oxford Science Publications, Oxford
5. Lehner KB, Rechl HP, Gmeinwieser JK, Heuck AF, Lukas HP, Kohl HP (1989) Structure, function and degeneration of bovine hyaline cartilage: assessment with MR imaging in vitro. Radiology 170:495–499
6. Modl JM, Sether LA, Haughton VM, Kneeland JB (1991) Articular cartilage: correlation of histologic zones with signal intensity at MR imaging. Radiology 181:853–855
7. Recht MP, Kramer J, Marcelis S, Pathria MN, Trudell D, Haghighi P, Sartoris DJ, Resnick D (1993) Abnormalities of articular cartilage in the knee: analysis of available MR techniques. Radiology 187:473–478
8. Chalkias SM, Pozzi-Mucelli RS, Pozzi-Mucelli M, Frezza F, Longo R (1994) Hyaline articular cartilage: relaxation times, pulse-sequence parameters and MR appearance at 1.5 T. Eur Radiol 4:353–359
9. Mlynárik V, Degrassi A, Toffanin R, Vittur F, Cova M, Pozzi-Mucelli RS (1996) Investigation of laminar appearance of articular cartilage by means of magnetic resonance microscopy. Magn Reson Med 14:435–442
10. Freeman DM, Bergman G, Glover G (1997) Short TE MR microscopy: accurate measurement and zonal differentiation of normal hyaline cartilage. Magn Reson Med 38:72–81
11. Waldschmidt JG, Rilling MJ, Kajdacsy-Balla AA, Boynton MD, Erickson SJ (1997) In vitro and in vivo MR imaging of hyaline cartilage: zonal anatomy, imaging pitfalls, and pathologic conditions. Radiographics 17:1387–1402
12. Rubenstein J, Recht M, Disler D, Kim J, Henkelman RM (1997) Laminar structures on MR images of articular cartilage. Radiology 204:15–16
13. Cova M, Toffanin R, Frezza F, Pozzi-Mucelli M, Mlynarik V, Pozzi-Mucelli RS, Vittur F, Dalla-Palma L (1998) Magnetic resonance imaging of articular cartilage: ex vivo study on normal cartilage correlated with magnetic resonance microscopy. Eur Radiol 8:1130–1136
14. Erickson SJ, Waldschmidt JG, Czervionke LF, Prost RW (1996) Hyaline cartilage: truncation artifact as a cause of trilaminar appearance with fat-suppressed three-dimensional spoiled gradient-recalled sequences. Radiology 201:260–264
15. Xia Y, Farquhar T, Burton-Wurster N, Lust G (1997) Origin of cartilage laminae in MRI. J Magn Reson Imaging 7:887–894
16. Xia Y (2000) Heterogeneity of cartilage laminae in MR imaging. J Magn Reson Imaging 11:686–693
17. Rubenstein J, Kim JK, Morava-Protzner I, Stanchev PL, Henkelman RM (1993) Effects of collagen orientation on MR imaging characteristics of bovine articular cartilage. Radiology 188:219–226
18. Erickson SJ, Prost RW, Timins ME (1993) The “magic angle” effect: background physics and clinical relevance. Radiology 188:23–25
19. Xia Y, Farquhar T, Burton-Wurster N, Ray E, Jelinski LW (1994) Diffusion and relaxation mapping of cartilage-bone plugs and excised disks using microscopic magnetic resonance imaging. Magn Reson Med 31:273–282
20. Recht MP, Resnick D (1994) MR imaging of articular cartilage: current status and future directions. Am J Roentgenol 163:283–290
21. Frank LR, Brossmann J, Buxton RB, Resnick D (1997) MR imaging truncation artifacts can create a false laminar appearance in cartilage. Am J Roentgenol 168:547–554
22. Xia Y (2000) Magic-angle effect in magnetic resonance imaging of articular cartilage. Invest Radiol 35:602–621
23. Henkelman RM, Stanisz GJ, Kim JK, Bronskill MJ (1994) Anisotropy of NMR properties of tissues. Magn Reson Med 32:592–601
24. Xia Y (1998) Relaxation anisotropy in cartilage by NMR microscopy (μMRI) at 14-μm resolution. Magn Reson Med 39:941–949
25. Gründer W, Wagner M, Werner A (1998) MR-microscopic visualization of anisotropic internal cartilage structures using the magic angle technique. Magn Reson Med 39:376–382
26. Kim DJ, Suh J, Jeong E, Shin K, Yang WI (1999) Correlation of laminated MR appearance of articular cartilage with histology, ascertained by artificial landmarks on the cartilage. J Magn Reson Imaging 10:57–64
27. Rubenstein JD, Kim JK, Henkelman RM (1996) Effects of compression and recovery on bovine articular cartilage: appearance on MR images. Radiology 201:843–850
28. Gründer W, Kanowski M, Wagner M, Werner A (2000) Visualization of pressure distribution within loaded joint cartilage by application of angle-sensitive NMR microscopy. Magn Reson Med 43:884–891
29. Wolff SD, Chesnick S, Frank JA, Lim KO, Balaban RS (1991) Magnetization transfer contrast: MR imaging of the knee. Radiology 179:623–628
30. Yao L, Sinha S, Seeger LL (1992) MR imaging of joints: analytic optimization of GRE techniques at 1.5 T. Am J Roentgenol 158:339–345
31. Disler DG, Peters TL, Muscoreil SJ, Ratner LM, Wagle WA, Cousins JP, Rifkin MD (1994) Fat-suppressed spoiled GRASS imaging of knee hyaline cartilage: technique optimization and comparison with conventional MR imaging. Am J Roentgenol 163:887–892
32. Disler DG, McCauley TR, Kelman CG, Fuchs MD, Ratner LM, Wirth CR, Hospodar PP (1996) Fat-suppressed three-dimensional spoiled gradient-echo MR imaging of hyaline cartilage defects in the knee: comparison with standard MR imaging and arthroscopy. Am J Roentgenol 167:127–132
33. Brossmann J, Frank LR, Pauly JM, Boutin RD, Pedowitz RA, Haghighi P, Resnick D (1997) Short echo time projection reconstruction MR imaging of cartilage: comparison with fat-suppressed spoiled GRASS and magnetization transfer contrast MR imaging. Radiology 203:501–507
34. Cova M, Toffanin R, Szomolanyi P, Vittur F, Pozzi-Mucelli RS, Jellus V, Silvestri F, Dalla-Palma L (2000) Short-TE projection reconstruction MR microscopy in the evaluation of articular cartilage thickness. Eur Radiol 10:1222–1226
35. Poole AR (1999) An introduction to the pathophysiology of osteoarthritis. Front Biosci 4:D662–D670
36. Paul PK, O'Byrne E, Blancuzzi V, Wilson D, Gunson D, Douglas FL, Wang JZ, Mezrich RS (1991) Magnetic resonance imaging reflects cartilage proteoglycan degradation in the rabbit knee. Skeletal Radiol 20:31–36

37. Loeuille D, Gonord P, Guingamp C, Gillet P, Blum A, Sauzade M, Netter P (1997) In vitro magnetic resonance microimaging of experimental osteoarthritis in the rat knee joint. J Rheumatol 24:133–139
38. Toffanin R, Mlynarik V, Russo S, Szomolanyi, Piras A, Vittur F (2001) Proteoglycan depletion and magnetic resonance parameters of articular cartilage. Arch Biochem Biophys 390:238–242
39. Burstein D, Gray ML, Hartman AL, Gipe R, Foy BD (1993) Diffusion of small solutes in cartilage as measured by nuclear magnetic resonance (NMR) spectroscopy and imaging. J Orthop Res 11:465–478
40. Xia Y, Farquhar T, Burton-Wurster N, Vernier-Singer M, Lust G, Jelinski LW (1995) Self-diffusion monitors degraded cartilage. Arch Biochem Biophys 323:323–328
41. Duvvuri U, Reddy R, Patel SD, Kaufman JH, Kneeland JB, Leigh JS (1997) $T_{1\rho}$-relaxation in articular cartilage: effects of enzymatic degradation. Magn Reson Med 38:863–867
42. Bashir A, Gray ML, Hartke J, Burstein D (1999) Nondestructive imaging of human cartilage glycosaminoglycan concentration by MRI. Magn Reson Med 41:857–865
43. Lesperance LM, Gray ML, Burstein D (1992) Determination of fixed charge density in cartilage using nuclear magnetic resonance. J Orthop Res 10:1–13
44. Insko EK, Reddy R, Leigh JS (1997) High-resolution, short echo time sodium imaging of articular cartilage. J Magn Reson Imaging 7:1056–1059
45. Reddy R, Insko EK, Noyszewski EA, Dandora R, Kneeland JB, Leigh JS (1998) Sodium MRI of human articular cartilage in vivo. Magn Reson Med 39:697–701
46. Borthakur A, Shapiro EM, Beeers J, Kudchodkar S, Kneeland JB, Reddy R (2000) Sensitivity of MRI to proteoglycan depletion in cartilage: comparison of sodium and proton MRI. Osteoarthritis Cartilage 8:288–293
47. Kim DK, Ceckler TL, Hascall VC, Calabro A, Balaban RS (1993) Analysis of water-macromolecule proton magnetization transfer in articular cartilage. Magn Reson Med 29:211–215
48. Gray ML, Burstein D, Lesperance LM, Gehrke L (1995) Magnetization transfer in cartilage and its constituent macromolecules. Magn Reson Med 34:319–325
49. Wachsmuth L, Juretschke HP, Raiss RX (1997) Can magnetization transfer magnetic resonance imaging follow proteoglycan depletion in articular cartilage? MAGMA 5:71–78
50. Bashir A, Gray ML, Burstein B (1996) Gd-DTPA^{2-} as a measure of cartilage degradation. Magn Reson Med 36:665–673
51. Allen RG, Burstein D, Gray ML (1999) Monitoring glycosaminoglycan replenishment in cartilage explants with gadolinium-enhanced magnetic resonance imaging. J Orthop Res 17:430–436
52. Bashir A, Gray ML, Boutin RD, Burstein D (1997) Glycosaminoglycan in articular cartilage: in vivo assessment with delayed Gd(DTPA)$^{2-}$ enhanced MR imaging. Radiology 205:551–558
53. Burstein D, Velyvis J, Scott KT, Stock KW, Kim Y, Jaramillo D, Boutin RD, Gray ML (2001) Protocol issues for delayed Gd(DTPA)$^{2-}$ enhanced MRI (dGEMRIC) for clinical evaluation of articular cartilage. Magn Reson Med 45:36–41
54. Bacic G, Liu KJ, Goda F, Hoopes PJ, Rosen GM, Swartz HM (1997) MRI contrast-enhanced study of cartilage proteoglycan degradation in the rabbit knee. Magn Reson Med 37:764–768
55. Wagner M, Werner A, Gründer W (1999) Visualization of collagenase-induced cartilage degradation using NMR microscopy. Invest Radiol 34:607–614